

EDGE-PRESERVING SMOOTHING OF HIGH-RESOLUTION IMAGES WITH A PARTIAL MULTIFRACTAL RECONSTRUCTION SCHEME

Jacopo Grazzini[†], Antonio Turiel[‡] and Hussein Yahia[†]

[†] Air Project
INRIA Rocquencourt
Domaine de Voluceau BP105 - 78153 Le Chesnay, France.
{jacopo.grazzini,hussein.yahia}@inria.fr

[‡] Departament de Física Fundamental
Universitat de Barcelona
Diagonal, 647 - 08028 Barcelona, Spain.
turiel@ffn.ub.es

KEY WORDS: High-resolution, Edge-preserving, Smoothing, Pre-segmentation, Multiscale, Multifractal, Singularity, Reconstruction.

ABSTRACT

The new generation of satellites leads to the arrival of very high-resolution images which offer a new quality of detailed information about the Earth's surface. However, the exploitation of such data becomes more complicated and less efficient as a consequence of the great heterogeneity of the objects displayed. In this paper, we address the problem of edge-preserving smoothing of high-resolution satellite images. We introduce a novel approach as a preprocessing step for feature extraction and/or image segmentation. The method is derived from the multifractal formalism proposed for image compression. This process consists in smoothing heterogeneous areas while preserving the main edges of the image. It is performed in 2 steps: 1) a multifractal decomposition scheme allows to extract the most informative subset of the image, which consists essentially in the edges of the objects; 2) a propagation scheme performed over this subset allows to reconstruct an approximation of the original image with a more uniform distribution of luminance. The strategy we adopt is described in the following and some results are presented for Spot acquisitions with spatial resolution of $20 \times 20 m^2$.

1 INTRODUCTION

In the latest years, the improvement of the technology for observing the Earth from the space has led to a new class of images with very high spatial resolution. New satellite sensors are getting closer to the spatial requirements, with, for example, resolutions of $2.5 m$ (Spot), $1 m$ (Ikonos) or even $0.7 m$ (QuickBird). High resolution (HR) imagery offers a new quality of detailed information about the properties of the Earth's surface together with their geographical relationships. Consequently, this has given rise to a growing interest on image processing tools and their application on this kind of images (Mather, 1995). Smaller and smaller objects (such as house plots, streets...), as well as precise contours of larger objects (such as field structures) are now available, automatic methods for extracting these objects are of great interest. However, due to the fact that HR images show great heterogeneity, standard techniques for analyzing, segmenting and classifying the data become less and less efficient. When the resolution increases, the spectral within-field variability also increases, which can affect the accuracy of further classification or segmentation schemes (Schiewe, 2002): images contain more complicated and detailed local textures; characteristic objects of the images (fields, buildings, rivers) are no more homogeneous. Thus, classical approaches cannot produce satisfactory results because they may induce simultaneously under- and over-segmentation within a single scene, depending on the heterogeneity of the considered objects, that confuse the global information and prevent further analysis. Generally several preprocessing steps may be required before such methods can be applied (Schowengerdt, 1997).

This paper introduces a new approach to edge-preserving smoothing of HR images as a preprocessing step for feature extraction and/or image segmentation. The problem can be related with the idea of resolution reduction: the retained technique should enable to preserve the features of the original image corresponding to the boundaries of the objects while homogeneizing the other parts (non-edges) of the image. Recently, Laporterie-Déjean *et al.* (Laporterie-Djean *et al.*, 2003) proposed a multiscale method for pre-segmenting HR images. The algorithm consists in performing a non-exact reconstruction: it decomposes and partially reconstructs images using morphological pyramids that enable to extract details which regard their structures within the image.

Like in (Laporterie-Djean *et al.*, 2003), we address this problem with a method derived from data compression. We use the multifractal approach introduced in (Turiel and Parga, 2000) as a resolution-reducing device. Like many image processing techniques, it makes use of the image edge information that is contained in the image gradient. Such an approach is ideal, as it assumes that objects can be reconstructed from their boundary information (Turiel and del Pozo, 2002). Moreover, it constitutes a multiscale approach which is well recognized to attain the best performance in processing purposes over satellite data, like image fusion and image merging (Yocki, 1995). Even on a single scene, different scales of analysis are needed, depending on the homogeneity of the objects under consideration and on the desired final application. The process we finally propose is done in two steps:

- First, meaningful subsets of the original image, which mainly consists in its boundaries, are extracted using

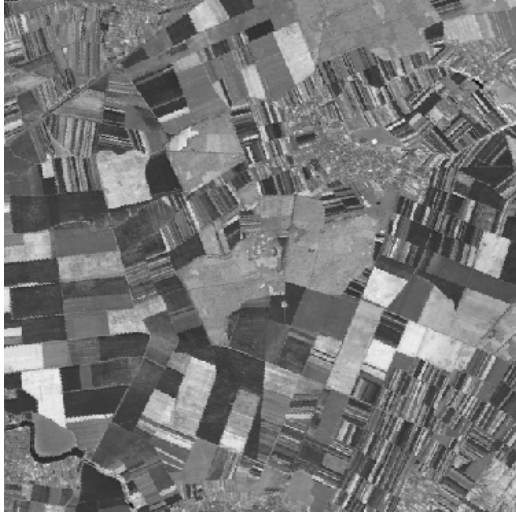


Figure 1: High-resolution **Spot** image ($20 \times 20 m$ per pixel) acquired in the Near Infrared channel. In this scene, we can recognize some fields, roads and also poorly delimited areas which correspond to cities.

a multifractal decomposition scheme.

- Second, an universal propagation kernel is used to partially reconstruct typical object shapes from the values of the gradient of the original image over the previous subset.

The paper is organized as follows. In section 2, we review the multifractal approach for extracting the meaningful entities in the images. In section 3, we introduce the method for reconstructing the images. We show that this method provides good results on Spot images with spatial resolution of $20 \times 20 m^2$ (see Fig. 1) and that it could be applied to any kind of data. We also consider an alternative version of this method. As a conclusion, we will discuss the advantages of our methodology.

2 THE MULTIFRACTAL DECOMPOSITION AND THE MSM

Multifractality is a property of turbulent-like systems which is generally reported on intensive, scalar variables of chaotic structure (Frisch, 1995). However, methods based on this approach have also shown to produce meaningful results in the context of real world images where irregular graylevel transitions are analyzed (Turiel and Parga, 2000). Natural images can be characterized by their singularities, *i.e.* the set of pixels over which the most drastic changes in graylevel value occur. In (Turiel and Parga, 2000), Turiel and Parga introduced a novel technique based on multifractal formalism to analyze these singularities. We develop in the following the basis of this technique.

In this approach, the points in a given image are hierarchically classified according to the strength of the transition of the image around them. The first step concerns the definition of an appropriate *multifractal measure*. Let us de-

note I an image and $\vec{\nabla}I$ its spatial derivative. We then define a measure μ through its density $d\mu(\mathbf{x}) = dx |\nabla I|(\mathbf{x})$, so that the measure of a ball $B_r(\mathbf{x})$ of radius r centered around the point \mathbf{x} is given by:

$$\mu(B_r(\mathbf{x})) = \int_{B_r(\mathbf{x})} dy |\nabla I|(\mathbf{y}). \quad (1)$$

Here $|\nabla I|$ denotes the modulus of the gradient $\vec{\nabla}I$. This measure gives an idea of the local variability of the graylevel values around the point \mathbf{x} . It was observed that for a large class of natural images, such a measure is multifractal (Turiel and Parga, 2000), *i.e.* the following relation holds:

$$\mu(B_r(\mathbf{x})) \sim \alpha(\mathbf{x}) r^{2+h(\mathbf{x})}. \quad (2)$$

All the scale dependance in eq. (2) is provided by the term $r^{2+h(\mathbf{x})}$ where the exponent $h(\mathbf{x})$ depends on the particular point considered. This exponent is called *singularity exponent* and quantifies the multifractal behaviour of the measure μ . The second step of the approach regards the estimation of these local exponents. This is done through a wavelet projection μ (Daubechies, 1992) of the measure, for which the same kind of relation as eq. (2) holds in a continuous framework, so that the exponents $h(\mathbf{x})$ can be easily retrieved. The reader is referred to (Turiel and Parga, 2000) for a full description of the method. By this way, each pixel \mathbf{x} of the image can be assigned a feature which measures the local degree of regularity of the signal $\vec{\nabla}I$ at this point. The singularity exponents computed on the Spot image of the Fig. 1 are represented in the Fig. 2. We see that the lowest values of singularity are mainly concentrated near the boundaries of the objects of the image (large culture fields in the middle part, roads in the lower left part). Some of them are also visible inside the culture fields, as they are not completely flatly illuminated, and in city areas (upper right part) that are rather heterogeneous.

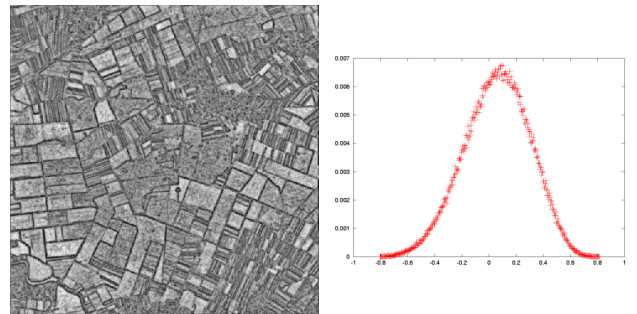


Figure 2: **Left:** representation of the singularity exponents computed on the image of the Fig. 1 in the range $[0, 255]$ of graylevel values; the brighter the pixel, the greater the singularity exponent at this point. **Right:** corresponding distribution of the singularity exponent; the range of values obtained is $[-0.80, 0.81]$.

The image can then be hierarchically decomposed in different subsets F_h gathering the pixels of similar features:

$$F_h \equiv \{\mathbf{x} \mid h(\mathbf{x}) \approx h\}. \quad (3)$$

We know, from the multifractal theory, that each one of these subsets is fractal, *i.e.* it exhibits the same geomet-

rical structure at different scales. In particular, the arising decomposition allows isolating a meaningful fractal component, the so-called MSM (*Most Singular Component*, denoted F_∞) associated with the strongest singularities (*i.e.* the lowest - or most negative - exponent, denoted h_∞). In Fig. 3, the MSM was computed on the original image at a rather coarse resolution: the pixels for which $h_\infty = -0.42 \pm 0.3$ were included in the MSM. From information theory, the MSM can be interpreted as the most relevant, informative set in the image (Turiel and del Pozo, 2002). In (Grazzini et al., 2002), Grazzini *et al.* have evidenced that this subset, computed on meteorological satellite data, is related with the maxima of some well-defined local entropy. From multifractal theory, the MSM can be regarded as a *reconstructing manifold*. In (Turiel and del Pozo, 2002), Turiel and del Pozo have shown that using only the information contained by the MSM, it is possible to predict the value of the intensity field at every point. We describe the algorithm for reconstructing images in the next section and we show that it can be used as a technique for edge-preserving smoothing of images.

3 THE RECONSTRUCTED IMAGES

In (Turiel and del Pozo, 2002), Turiel and del Pozo proposed an algorithm supposed to produce a perfect reconstruction FRI (*Fully Reconstructed Image*) from the MSM. The authors introduced a rather simple vectorial kernel \vec{g} capable to reconstruct the signal I from the value of its spatial gradient $\vec{\nabla}I$ over the MSM. Namely, let us define the density function $\delta_\infty(\mathbf{x})$ of the subset F_∞ which equals 1 if $\mathbf{x} \in F_\infty$ and 0 if $\mathbf{x} \notin F_\infty$. Let also define the gradient restricted to the same set $\vec{v}_\infty \equiv \vec{\nabla}I \delta_\infty$, *i.e.* the field which equals the gradient of the original image over the MSM and is null elsewhere: this will be the only data required for the reconstruction. The reconstruction formula is then expressed as:

$$I(\mathbf{x}) = \vec{g} \star \vec{v}_\infty(\mathbf{x}) \quad (4)$$

where \star denotes the convolution. The reconstruction kernel \vec{g} is easily represented in Fourier space by:

$$\hat{\vec{g}}(\mathbf{f}) = i \mathbf{f} / |\mathbf{f}|^2 \quad (5)$$

where $\hat{\cdot}$ stands for the Fourier transform, \mathbf{f} denotes the frequency and i the imaginary unit. The principle is that of a propagation of the values of the signal $\vec{\nabla}I$ over the MSM to the whole image. The full algorithm for reconstruction is given in (Turiel and del Pozo, 2002).

The multifractal model described above also allows to consider a related concept, that of RMI (*Reduced Multifractal Image*), as it was introduced in (Grazzini et al., 2002). It consists in propagating, through the same reconstruction formula (4), instead of \vec{v}_∞ , another field \vec{v}_0 so that a more uniform distribution of the luminance in the image is obtained. Namely, the field \vec{v}_0 is simply built by assigning to every point in the MSM an unitary vector, perpendicular to the MSM and with the same orientation as the original gradient $\vec{\nabla}I$. Thus, by introducing in eq. (4) this rather naive vector field, we obtain the RMI. Consequently, the

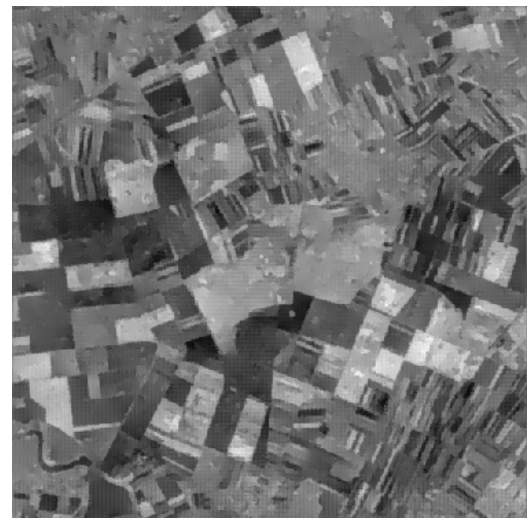
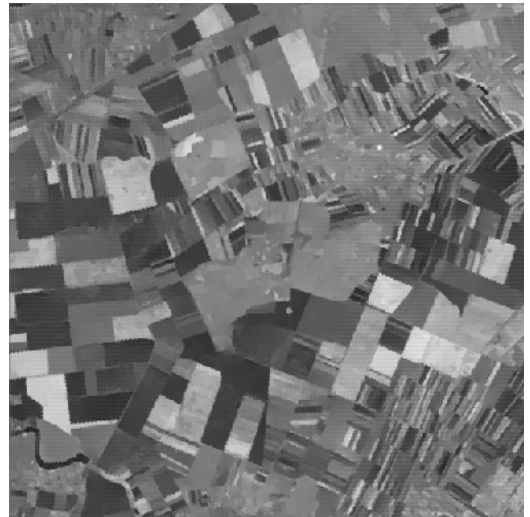
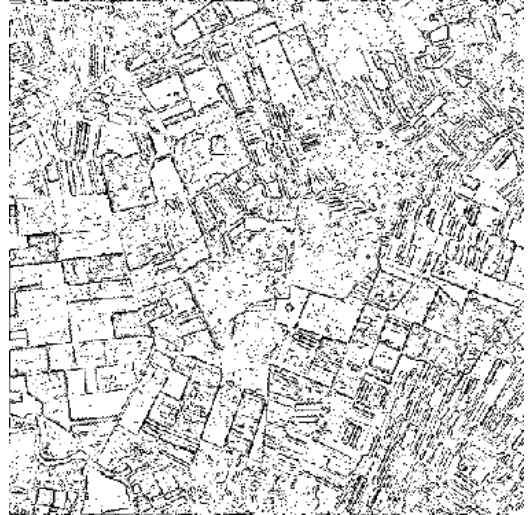


Figure 3: **Top:** MSM (dark pixels) extracted at $h_\infty = -0.42 \pm 0.3$ from the image of Fig. 1; quantitatively, the MSM gathers 22.29% of the pixels of the image. **Middle:** FRI computed with eq. (4) on the field \vec{v}_∞ ($PSNR = 24.93 \text{ dB}$). **Bottom:** RMI computed with the field \vec{v}_0 ($PSNR = 21.34 \text{ dB}$).

RMI has the same multifractal exponents (and so, the same MSM) as the original image, but, as desired, a more uniform graylevel distribution. In fact, this image ideally attains the most uniform distribution of graylevels compatible with the multifractal structure of the original image. RMI images define smaller (*i.e.*, more compressed) codes than FRI images; both images are very similar when the original images are uniformly illuminated.

In Fig. 3, we present the images reconstructed from the fields \vec{v}_∞ and \vec{v}_0 defined by the MSM previously computed (see section 2). This approximates the original image of Fig. 1 with a *Peak Signal to Noise Ratio (PSNR)* of 24.93 dB and $PSNR = 21.34$ dB respectively.

4 DISCUSSION

From the whole reconstructions displayed in Fig. 3 and the details displayed in Fig. 4, we see that:

- for both reconstructions, there is a high degree of smoothing in rather homogeneous areas,
- main edges are preserved, even those ones being represented by small gray value changes, like inside the culture fields,
- even if it may happen that edges between small areas are deleted, like for small culture fields, small homogeneous regions are generally conserved.

The similarity between both reconstructions is mainly due to the fact that on this kind of images (namely, land cover images with rather linear edges induced by culture fields) the field \vec{v}_0 does not strongly deviate from the field \vec{v}_∞ . So, in first approximation, the RMI could be used for providing the information about the boundaries. However, the corresponding graylevel distributions (Fig. 4) show that:

- the FRI provides a good smoothed version of the original image, with suppression of peaks in the distribution,
- the RMI provides a completely different chromatic distribution.

The RMI represents a different, possible view of the same scene, with the same objects and the same geometry as the FRI, but different distributed illumination of each part. Namely, the differences between the RMI and the original image are only due to these differences in illumination. In spite of the advantages of a more compact code as the one associated to the RMI, we finally retain the FRI as the convenient edge-preserving smoothing approximation of the original image: it cleans up noise in the homogeneous areas but preserves important structures and also preserves the luminance distribution. Besides, the quality of the approximation of the original image is good for the FRI, which is an essential requirement for further processing like feature extraction. Close inspection to the image

also shows that the method is able to enhance subtle texture regions, like small culture fields. It is clear that the results are superior to the results of a simple method like pixel averaging for instance.

Now, one of the major advantages of our method of pre-segmentation is that it is parameterizable. We should notice that the reconstruction algorithm for computing the FRI defined by the eq. (4) is linear (Turiel and del Pozo, 2002). It means that, if the reconstructing manifold is the union of two subsets $\varphi_1 \cup \varphi_2$, then the $FRI_{\varphi_1 \cup \varphi_2}$ reconstructed from this manifold equals the addition of the FRI_{φ_1} and FRI_{φ_2} reconstructed from each part separately. Thus, the more singular pixels the reconstructing manifold gathers, the closer to the original image the FRI is. In particular, when the MSM consists of all the points in the image, eq. (4) becomes a trivial identity and the reconstruction is perfect. So, we can approximate the original image as close as desired. We just need to choose the density of the manifold used for the reconstruction, *i.e.* we need to adjust the range of values accepted for the singularity exponents of the pixels belonging to the MSM. By this way, the degree of smoothing of objects in the image can be controlled. On the Fig. 5, we see that the details of the image are incorporated in the reconstruction when increasing the authorized number of pixels in the MSM, and this is done gradually, according to their degree of singularity.

5 CONCLUSION

In this paper, we have proposed to perform a pre-segmentation of high resolution images prior to any processing. For this purpose, we adopt an approach related with data compression and based on the multifractal analysis of images. The main idea is that of a partial reconstruction process of the images from the extraction of their most important features.

The multifractal algorithm is performed in two steps, which consist in: first, extracting the most singular subset of the image, *i.e.* the set of pixels where strong transitions of the original image occur, and, then, performing a reconstruction by propagating the graylevel values of the spatial gradient of the image from this subset to the other parts. The multiscale character of the extraction step allows to retain the relevant edges, no matter at which scale they happen, and without significant artifacts. The most singular subset is mainly composed of pixels belonging to the boundaries of the objects in the image. So that, our algorithm to reconstruct images is consistent with classical hypothesis stating that edges are the most informative parts of the image (Marr, 1982). The quality of the reconstruction depends on the validity of the hypothesis defining the reconstruction kernel and in the accuracy of the edge detection step. It should be also noticed that this method can be used as a starting point for a coding scheme, as it retains the most meaningful features of the image.

The reconstruction strategy results in very nicely smoothed homogeneous areas while it preserves the main information contained in the boundaries of objects. It is good at

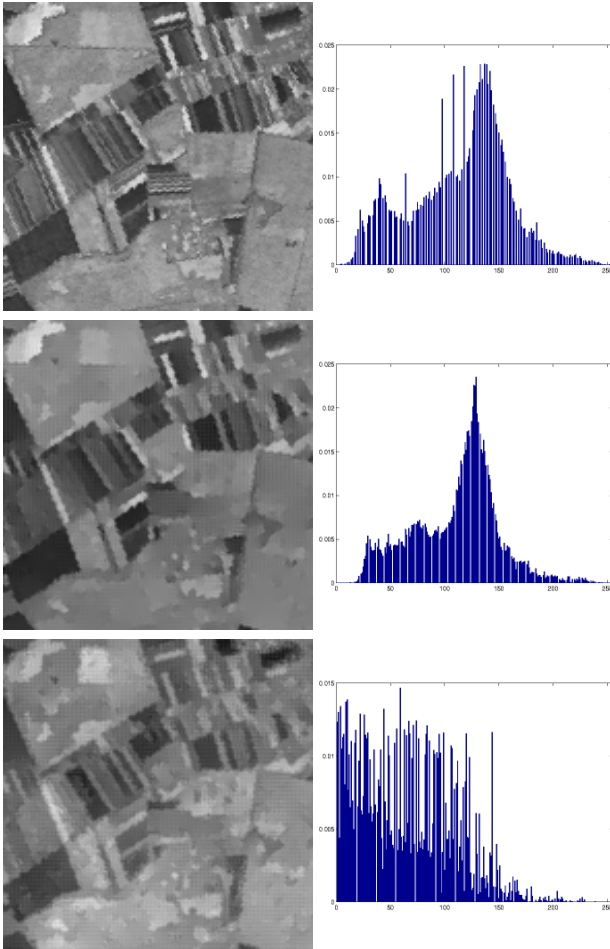


Figure 4: Details of the reconstructed images and their graylevel values' distribution. **From top to bottom:** details of the original Spot image, details of the FRI and the RMI, respectively reconstructed with the fields \vec{v}_∞ and \vec{v}_0 .

enhancing textures, as it smoothens the image, and, thus, suppresses small elements corresponding to the main heterogeneity. The image structures are not geometrically damaged, what might be fatal for further processings like classification or segmentation. Indeed, it creates homogeneous regions instead of points or pixels as carriers of features which should be introduced in further processing stages. Moreover, the reconstruction is parameterizable. The fidelity to the original image can be adjusted, by gradually incorporating as many details of the original image as desired, so that the degree of smoothing can be controlled. As a continuation, we intend, for a deeper validation of the method, to perform the algorithm on very high resolution images.

ACKNOWLEDGMENT

J. Grazzini is funded by a grant from the *Regional Council of Île-de-France* (agreement no. E.1358). A. Turiel is funded by a contract RED2002 from Generalitat de Catalunya.

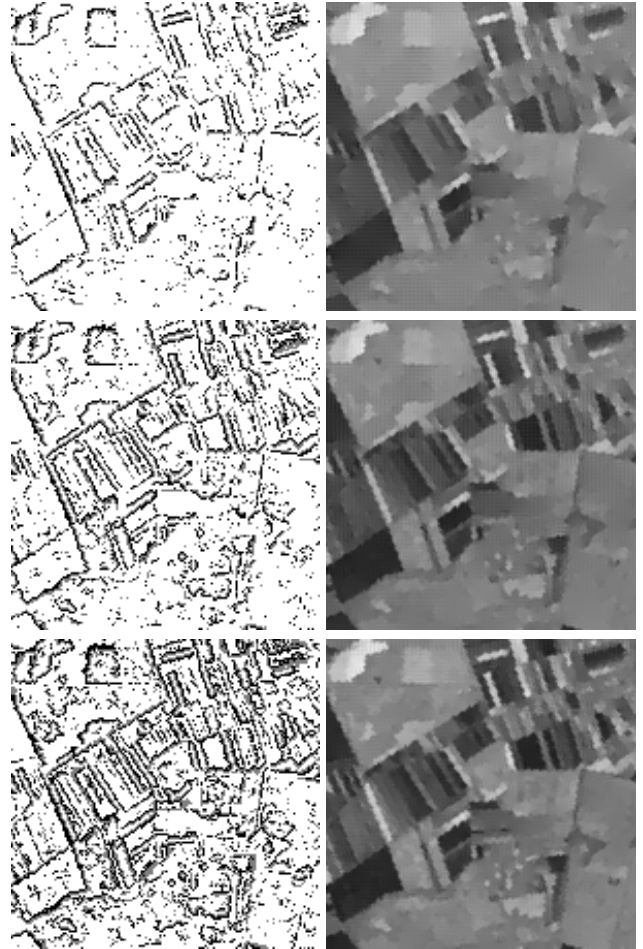


Figure 5: FRI obtained considering different MSM with varying density in the image. **From top to bottom:** 13.9% and $PSNR = 23.51 \text{ dB}$, 22.3% and $PSNR = 24.93 \text{ dB}$, 32.5% and $PSNR = 25.30 \text{ dB}$ (the $PSNR$ were computed for the whole images). Note that the middle image is the same as the middle one displayed in Fig. 4

REFERENCES

- Daubechies, I., 1992. Ten lectures on wavelets. CBMS-NSF Series in Appl. Math., Capital City Press, Philadelphia (USA).
- Frisch, U., 1995. Turbulence. The Legacy of Kolmogorov. Cambridge University Press, Cambridge MA.
- Grazzini, J., Turiel, A. and Yahia, H., 2002. Entropy estimation and multiscale processing in meteorological satellite images. In: Proc. of ICPR, Vol. 3, pp. 764–768.
- Laporterie-Djean, F., Lopez-Ornelas, E. and Flouzat, G., 2003. Pre-segmentation of high-resolution images thanks to the morphological pyramid. In: Proc. of IGARSS, Vol. 3, pp. 2042–2044.
- Marr, D., 1982. Vision. W.H. Freeman and Co., New York.
- Mather, P., 1995. Computer Processing of Remotely-Sensed Images: An Introduction. John Wiley & Sons, Chichester (UK). 2nd ed.

Schiewe, J., 2002. Segmentation of high-resolution remotely sensed data - concepts, applications and problems. *Int. Arch. of Photogrammetry and Remote Sensing* 34(4), pp. 380–385.

Schowengerdt, R., 1997. *Remote Sensing. Models and Methods for Image Processing*. Academic Press, San Diego (USA).

Turiel, A. and del Pozo, A., 2002. Reconstructing images from their most singular fractal set. *IEEE Trans. on Im. Proc.* 11, pp. 345–350.

Turiel, A. and Parga, N., 2000. The multi-fractal structure of contrast changes in natural images: from sharp edges to textures. *Neural Comp.* 12, pp. 763–793.

Yocki, D., 1995. Image merging and data fusion by means of the discrete 2D wavelet transform. *J. Opt. Soc. Am. A* 12(9), pp. 1834–1841.